of the Method of Grids in Gas Dynamics [in Russian], Moscow State University Press, Moscow (1971), No. 1.
13. W. D. Hayes and R. F. Probstein, Hypersonic Flow Theory, 2nd ed., Academic Press, New York (1967).

FLOW IN A CHANNEL WITH SUCTION ON ONE SIDE: DETACHMENT FROM AN IMPERMEABLE WALL AND EFFECT OF ROTATION AROUND THE TRANSVERSE AXIS

S. A. Vasil'ev and E. M. Smirnov

UDC 532.516

1. Plane Flow: Review of Formulations and Results. We shall study the plane flow of a viscous incompressible liquid along a channel formed by two parallel walls, under conditions such that one is impermeable and liquid is suctioned uniformly through the other wall. We denote the distance between the walls by H. We shall assume that the flow occurs in the yOz plane; we place the origin of the Cartesian coordinate system in the inlet section on the impermeable wall and we orient the z-axis parallel to the walls in the direction of the flow. The equations of motion and continuity have the form

$$w\frac{\partial w}{\partial z}+v\frac{\partial w}{\partial y}=-\frac{1}{\rho}\frac{\partial p}{\partial z}+\nu\left(\frac{\partial^2 w}{\partial z^2}+\frac{\partial^2 w}{\partial y^2}\right),$$
$$w\frac{\partial v}{\partial z}+v\frac{\partial v}{\partial y}=-\frac{1}{\rho}\frac{\partial p}{\partial y}+\nu\left(\frac{\partial^2 v}{\partial z^2}+\frac{\partial^2 v}{\partial y^2}\right),\quad \frac{\partial w}{\partial z}+\frac{\partial v}{\partial y}=0. \tag{1.1}$$

The solution of the equations must satisfy the boundary conditions

$$y=0:\ w=v=0;\quad y=H:\ w=0,\ v=v_s \tag{1.2}$$

($v_s > 0$ is the suction velocity).

In [1, 2] it is shown that the system (1.1) can have a self-similar solution of the form

$$w=(W_m-v_s z/H)f'(\eta),\ v=v_s f(\eta). \tag{1.3}$$

Here W_m is the mean flow at the inlet; $\eta = y/H$. For the problem at hand the function $f(\eta)$ satisfies the equation

$$f'''+\mathrm{R}_s(f'^2-ff'')=k \tag{1.4}$$

and the boundary conditions

$$f(0)=f'(0)=0,\ f(1)=1,\ f'(1)=0. \tag{1.5}$$

One of the boundary conditions is used to find the constant k which determines the longitudinal pressure gradient. The parameter of the self-similar solution is Reynolds number $\mathrm{R}_s=v_sH/\nu$, contructed based on the suction velocity. In [3] the problem (1.4) and (1.5) is solved analytically by the method of expansion in a series in powers of R_S and the solution is valid for small values of this parameter. We do not know of any other solutions of the self-similar problem.

The solutions of the two-dimensional problem (1.1) and (1.2) were found by the finite-difference method in [4]. The purpose of the calculations was to study the flow field in a flat heat pipe. The downstream end of the pipe was assumed to be closed. The conditions at the inlet into the suctioned section (condenser section) were not fixed; they were determined

Leningrad. Translated from Zhurnal Prikladnoi Mekhaniki i Tekhnicheskoi Fiziki, No. 5, pp. 66-71, September-October, 1989. Original article submitted May 11, 1988.

0021-8944/89/3005-0731$12.50 © 1990 Plenum Publishing Corporation

TABLE 1

R_s	η_*	$-f_*$	R_s	η_*	$-f_*$
14	0,134	0,0026	18	0,430	0,874
14,4 (I)	0,211	0,0112	20	0,426	0,954
14,4 (II)	0,375	0,134	30	0,416	1,133
14,4 (III)	0,431	0,537	40	0,405	1,207
16	0,433	0,744			

by the character of the flow in other sections. The results presented nonetheless show that in all cases the inlet profile is close to a Poiseuille parabola. The length of the suctioned section was 100H/3, and R_S assumed values from 1 to 50. Differences from flow in a channel with impermeable walls are already perceived for $R_S = 2$. For $R_S = 20$ and 50 detachment arises approximately midway above the channel and for $R_S = 50$ it already develops in the first cell of the computing grid (we note that there are only nine steps of the grid on the entire suctioned section).

In [3] the problem of flow development in a channel suctioned on one side is studied based on parabolized equations of motion; the pressure is assumed to be constant in each transverse section. The dependence of the coordinate of the point of detachment of the flow on R_S for two types of inlet profile – uniform and parabolic – is presented as the main result of the calculations.

2. Plane Flow: New Results. The main goal of this work is to study three-dimensional flow numerically. In so doing we have obtained a number of new results pertaining to plane flows. This permitted comparing plane and three-dimensional flows under comparable conditions.

The self-similar problem (1.4) and (1.5) was reduced to a Cauchy problem and solved numerically. The calculations showed that $f''(0)$ vanishes for $R_s = R_s^* = 13.13$. The profiles of the longitudinal component of the velocity with a section of return flow correspond to higher values of R_S. We note that the analytical solution of [3], including terms in the series with the zeroth and first powers of the parameter R_S, gives $R_S^* = 13.12$. Such good agreement with the numerical solution is somewhat unexpected, since the applicability of this analytical solution is, strictly speaking, limited to small values of R_S. Table 1 gives the values of the coordinate $\eta = \eta_*(R_s)$ for which $f'(\eta)$ changes sign; the interval $0 < \eta < \eta_*$ corresponds to the section with return flow; the values of $f_* = f(\eta = \eta_*)$ are also given. The ratio $|f_*|/(1 + |f_*|)$ can be regarded as a quantitative characteristic of the intensity of the return flow. We note that the depdences $\eta_*(R_S)$, $f_*(R_S)$ have two turning points, the first of which corresponds to $R_S = 14.5$ (turning toward lower values of R_S) while the second one corresponds to $R_S = 14.1$ (turning toward higher values of R_S). In the interval $14.1 < R_S < 14.5$ η_* and f_* each have three values; this situation is illustrated in Table 1 by the computational results for $R_S = 14.4$.

The problem (1.1) and (1.2) was integrated numerically using the scheme proposed in [5] (a similar scheme is described below in application to the three-dimensional problem). The calculations were performed for channels with length $L^0 = L/H = 5$ and 10, and the parameter R_S was varied from 2 to 50. A uniform velocity profile ($w = W_m$ and $v = 0$) was given at the inlet. The formulation of the problem was completed by the condition for sticking on the impermeable end wall. The difference grid with uniform steps contained 30 × 86 nodes. The calculations showed that for $2 \leq R_S \lesssim 12$ the flow at the impermeable wall contains near the endface a small region with a negative value of the longitudinal velocity component. Rapid growth of the size of the zone of return flow is observed starting with $R_S = 12$-14. It is interesting that $R_S^* = 13.13$, obtained in the self-similar solution, falls into the indicated range of values of R_S.

We shall characterize the dimensions of the zone of return flow by its length ℓ_r, defined as the distance from the point of detachment to the end wall, and the maximum width b_r. Table 2 gives the values of $l_r^0 = l_r/L$, $b_r^0 = b_r/H$ as a function of R_S and L^0; the values of $\ell_r{}^0$ based on the results of the solution of [3], obtained based on the parabolized equations of motion, are given for comparison. One can see from Table 2 that for $R_S \gtrsim 14$ the length of the channel L^0 has virtually no effect on $\ell_r{}^0$ and a stronger effect

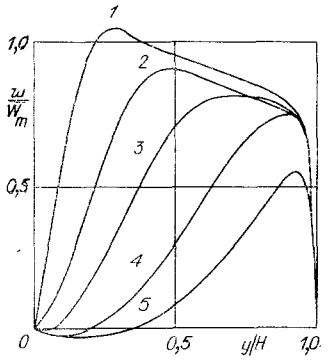

Fig. 1

on the width of the zone of return flow. In the same region of R_s the computed values of ℓ_r^0 are on the whole close to the results of [3]. Comparison with the data of [3, 4] shows that with a parabolic input profile w the detachment of flow from the impermeable wall develops for smaller values of z/L and, as a consequence, ℓ_r^0 is greater than for a uniform input profile.

Figure 1 shows profiles of the longitudinal component of the velocity in the channel $L^0 = 5$ with $R_s = 40$; the curves 1-5 correspond to z/H = 5/6, 5/3, 5/2, 10/3, and 25/6. In the first two sections the maximum of the velocity is shifted toward the impermeable wall. This is due to the fact that the boundary layers on the walls of the channel do not develop in the same way – the rapidly growing layer on the impermeable wall has a stronger displacing effect. Downstream the maximum of the velocity is shifted increasing more toward the wall with suction. The presented profiles and the profiles for other values of R_s show that in the zone of return flow the velocities are low. This result does not agree with the results following from the self-similar solution obtained for the same values of R_s.

3. Formulation of the Three-Dimensional Problem. The need for studies of three-dimensional flows in channels with a permeable wall arises, in particular, in connection with the development of new convective systems for cooling nozzles and working blades in high-temperature turbines. In a number of systems the cooling medium flows along radical channels in the blade and flows out into the interblade space through the permeable cladding of the blade. In the front part of the working blade, where the maximum heat fluxes occur, the permeable wall of the radial channel makes a nearly right angle with the rotation axis.

We shall study a flow in a channel with a square cross section H × H, which rotates with a constant angular velocity ω around the transverse axis. As before, we orient the z-axis of the Cartesian coordinate system Oxyz parallel to the walls of the channel in the direction of the flow; we orient the rotation axis parallel to the y-axis; and, liquid is suctioned through the wall perpendicular to this axis.

We write the equations for the steady-state relative motion in the dimensionless form, choosing for the scale the size H and average flow velocity W_m at the inlet into the channel:

$$(\mathbf{V}\cdot\nabla)\mathbf{V} = -\frac{1}{\rho}\operatorname{grad} p_* - 2K\frac{\boldsymbol{\omega}}{\omega}\times\mathbf{V} + \frac{1}{\mathrm{Re}}\Delta\mathbf{V}; \tag{3.1}$$

$$\operatorname{div}\mathbf{V} = 0. \tag{3.2}$$

Here $\mathbf{V}$ is the velocity vector with components u, v, and w, corresponding to the x, y, and z-axes; $p_* = p - \rho\omega^2 r^2/2$ is the modified pressure; r is the shortest distance to the rotation axis; $\mathrm{Re} = W_m H/\nu$ is the Reynold's number; and $K = \omega H/W_m$ is the rotation parameter.

The condition of sticking is imposed on all bounding impermeable walls and the distribution of the suction velocity $v_w(x, z)$ and the condition that two other components vanish are imposed on the permeable wall. In concrete situations the formulation of the problem is completed by giving conditions at the inlet and outlet from the channel or at the closed end.

4. Numerical Method. We shall briefly describe the method employed to find the numerical solutions, which is based on the method of stabilization combined with the method of artificial compressibility. A term with a derivative with respect to a fictitious stabilization time is introduced into Eq. (3.1), and the equation of continuity is written in the relaxational form $A\partial p_*/\partial t + \operatorname{div}\mathbf{V} = 0$ (A is an iteration parameter). The problem is then formulated

TABLE 2

R_s	$l_r^0=l_r/L$	$b_r^0=b_r/H$	$l_r^0=l_r/L$	$b_r^0=b_r/H$	$l_r^0=l_r/L$	$b_r^0=b_r/H$
	L^0					
	5		10		$\gg 1$ [3]	
10	0,05	0,13	0,02	0,11	0	—
12	0,07	0,16	0,04	0,15	0	—
14	0,12	0,25	0,10	0,23	0,09	—
16	0,20	0,27	0,20	0,29	0,18	—
18	0,27	0,31	0,27	0,34	0,27	—
20	0,32	0,35	0,32	0,40	0,32	—
30	0,48	0,48	0,49	0,55	0,47	—
40	0,55	0,57	0,57	0,62	0,54	—
50	0,60	0,63	0,62	0,65	0,60	—

relative to the increments of the vector $\mathbf{U} = \{u, v, w, p_*\}$ on the n-th time layer

$$\Delta\mathbf{U}^{n+1}/\Delta t + \Lambda^n(\mathbf{U}^n + \Delta\mathbf{U}^{n+1}) = 0, \tag{4.1}$$

where $\mathbf{U}^n$, $\Delta\mathbf{U}^{n+1}$ are the values of the vector $\mathbf{U}$ and its increment at the n-th time layer; Λ^n is a nonlinear matrix operator; and, Δt is a step along the fictitious time axis.

The equations (4.1) are linearized relative to the increments $\Delta\mathbf{U}^{n+1}$ and split with respect to the spatial coordinates:

$$\begin{aligned}
(E + \Delta t\Lambda_x^n)\,\Delta\mathbf{U}^{n+1/3} &= -\Delta t\Lambda^n\mathbf{U}^n,\\
(E + \Delta t\Lambda_y^n)\,\Delta\mathbf{U}^{n+2/3} &= \Delta\mathbf{U}^{n+1/3},\\
(E + \Delta t\Lambda_z^n)\,\Delta\mathbf{U}^{n+1} &= \Delta\mathbf{U}^{n+2/3}.
\end{aligned}$$

Here $\Delta\mathbf{U}^{n+1/3}$, $\Delta\mathbf{U}^{n+2/3}$ are the intermediate grid functions; Λ_x^n, Λ_y^n, Λ_z^n are the matrix operators of the equations of motion, written in a conservative form of fractional steps along the directions x, y, and z:

$$\Lambda_x^n = \begin{bmatrix}
\frac{\partial}{\partial x}\left(-\frac{1}{\mathrm{Re}}\frac{\partial}{\partial x} + 2u^n\cdot\right) & 0 & 0 & \frac{\partial}{\partial x}\\
\frac{\partial}{\partial x}(v^n\cdot) & \frac{\partial}{\partial x}\left(-\frac{1}{\mathrm{Re}}\frac{\partial}{\partial x} + u^n\cdot\right) & 0 & 0\\
\frac{\partial}{\partial x}(w^n\cdot) - 2K & 0 & \frac{\partial}{\partial x}\left(-\frac{1}{\mathrm{Re}}\frac{\partial}{\partial x} + u^n\cdot\right) & 0\\
\frac{1}{A}\frac{\partial}{\partial x} & 0 & 0 & 0
\end{bmatrix},$$

$$\Lambda_y^n = \begin{bmatrix}
\frac{\partial}{\partial y}\left(-\frac{1}{\mathrm{Re}}\frac{\partial}{\partial y} + v^n\cdot\right) & \frac{\partial}{\partial y}(u^n\cdot) & 0 & 0\\
0 & \frac{\partial}{\partial y}\left(-\frac{1}{\mathrm{Re}}\frac{\partial}{\partial y} + 2v^n\cdot\right) & 0 & \frac{\partial}{\partial y}\\
0 & \frac{\partial}{\partial y}(w^n\cdot) & \frac{\partial}{\partial y}\left(-\frac{1}{\mathrm{Re}}\frac{\partial}{\partial y} + v^n\cdot\right) & 0\\
0 & \frac{1}{A}\frac{\partial}{\partial y} & 0 & 0
\end{bmatrix},$$

$$\Lambda_z^n = \begin{bmatrix}
\frac{\partial}{\partial z}\left(-\frac{1}{\mathrm{Re}}\frac{\partial}{\partial z} + w^n\cdot\right) & 0 & \frac{\partial}{\partial z}(u^n\cdot) + 2K & 0\\
0 & \frac{\partial}{\partial z}\left(-\frac{1}{\mathrm{Re}}\frac{\partial}{\partial z} + w^n\cdot\right) & \frac{\partial}{\partial z}(v^n\cdot) & 0\\
0 & 0 & \frac{\partial}{\partial z}\left(-\frac{1}{\mathrm{Re}}\frac{\partial}{\partial z} + 2w^n\cdot\right) & \frac{\partial}{\partial z}\\
0 & 0 & \frac{1}{A}\frac{\partial}{\partial z} & 0
\end{bmatrix}.$$

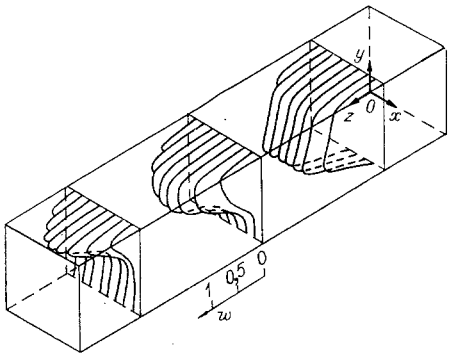

Fig. 2

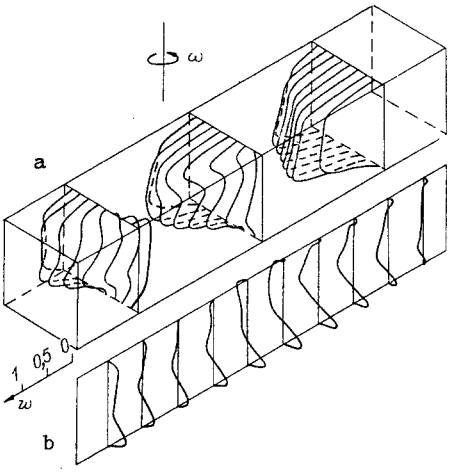

Fig. 3

The point in the tables of the operators denotes multiplication by the corresponding components of the columns $\Delta \mathbf{U}^{n+1/3}$, $\Delta \mathbf{U}^{n+2/3}$, $\Delta \mathbf{U}^{n+1}$. We stress that summing Λ_x^n, Λ_y^n, Λ_z^n does not give the operator Λ^n because the latter is nonlinear. The derivatives appearing in the operators are approximated by central differences on the grid of the method of markers and cells with shifted nodes. The vector $\mathbf{U}$ is sought as the stationary solution of Eqs. (4.1), satisfying the condition $\Lambda^n \mathbf{U}^n \leqslant \varepsilon$. The described difference scheme was essentially taken from [5]; the new element is that the action of the Coriolis force is taken into account.

In the problem at hand the effects owing to suction and rotation lead to large gradients of the velocity at the walls perpendicular to the y-axis. To improve the resolution of the numerical method a transformation to the new coordinate y_1, related with y by the relation

$$y = \frac{0.5 \operatorname{sign} y_1}{1 - \exp(-a)} [1 - \exp(-2a|y_1|)] + 0.5,$$

where a is the exponential transformation parameter and the coordinate y is measured from the impermeable wall while y_1 varies over the interval [-1/2, 1/2], was made in (3.1) and (3.2). As a result, the derivatives with respect to y in the operators Λ^n, Λ_y^n were replaced by the relations

$$\frac{\partial}{\partial y} = \frac{1 - \exp(-a)}{a} \exp(2a|y_1|) \frac{\partial}{\partial y_1},$$

$$\frac{\partial^2}{\partial y^2} = \left[\frac{1 - \exp(-a)}{a}\right]^2 \exp(4a|y_1|) \left(\frac{\partial^2}{\partial y_1^2} + 2a \operatorname{sign} y_1 \frac{\partial}{\partial y_1}\right).$$

5. Computational Results. The numerical solutions of the three-dimensional problem were found for a channel with length $L^0 = 5$. The condition of uniform suction was imposed on the wall with coordinate y = 1; the other walls were assumed to be impermeable, including also the end wall which terminated the channel. All results presented below were obtained on a 16 × 16 × 44 grid with the parameter of nonuniformity of the grid a = 1.4, Re = 200, and R_s = Re/5 = 40.

We shall first study flow in a nonrotating channel. Figure 2 shows the distributions of the longitudinal component of the velocity in three normal sections with the coordinates z = 5/6, 5/2, and 25/6 (at the inlet to the channel w is distributed uniformly). Like in the case of the plane flow, near the inlet to the channel the maximum of velocity is shifted toward the impermeable wall. Detachment develops downstream: a region with small negative velocities forms at the impermeable wall, and the direct flow is concentrated at the suctioned wall. In the middle plane $\ell_r^0 = 0.37$, which is less than in the plane flow. The displacement of the line of detachment downstream is obviously due to the displacing effect of the boundary layers on the side walls bounding the flow along the x-axis.

The calculations of the flow in a rotating channel were performed for K = 0.2, 0.4, and 0.6. For velocity components at the inlet to the channel the conditions u = 0, v = 0, and w = $1 + 2K(x - 1/2)$ were imposed; these conditions correspond to flow with nearly zero absolute vorticity at the channel inlet.

The flow field for K = 0.4 is illustrated in Fig. 3: a – the distributions w(x, y) for values of z indicated above for Fig. 2; b – the profiles u(y) in the middle plane x = const for values of z with a step of 10/21, starting with z = 25/84; the scale for w and u is the same. Comparing Fig. 3a with Fig. 2 shows that the effect of rotation is very significant. Detachment from the wall with coordinate y = 0 is suppressed, but a wide region of return flow at the side wall develops (x = 1 for the positive direction of rotation). As K increases there is a tendency for the field w to become uniform in the direction of the rotation axis (the y-axis); this tendency is characteristic for flows of rotating liquid, including for flows in rotating channels [6]. Figure 3b shows that flow of liquid in the direction of the x-axis plays an important role in the formation of the flow field.

The velocity level in the zone of return flow at the wall x = 1 is very significant; the maximum velocity of the return flow with K = 0.2, 0.4, and 0.6 is 27, 39, and 49% of W_m. The formation of this zone is a result of the summation of two effects: the acquiring of vorticity 2ω by the particles of fluid owing to interaction with the walls and intensification of the acquired vorticity by means of stretching of the vortex tubes by the superposed suction.

LITERATURE CITED

1. A. S. Berman, "Laminar flow in channels with porous walls," J. Appl. Phys., 24, No. 9 (1953).
2. R. M. Terril, "Possibility of the existence of a characteristic solution for a laminar flow in a channel with porous walls," Prikl. Mekh., 33, No. 1 (1966).
3. V. M. Eroshenko and L. I. Zaichik, Hydrodynamics and Heat Transfer on Impermeable Surfaces [in Russian], Nauka, Moscow (1984).
4. H. Van Owen and K. D. Hogendorn, "Calculations of vapor flows in a flat heat pipe," RTK, 17, No. 11 (1979).
5. Yu. É. Egorov and S. B. Koleshko, "Application of the method of fractional steps for numerical solution of the equations of an incompresisble viscous liquid in natural variables" in: Dynamics of Nonuniform and Compressible Media [in Russian], Leningrad State University, Leningrad (1984), No. 8.
6. E. M. Smirnov and S. V. Yurkin, "Discussion of fluid flow along a rotating channel with a square transverse cross section," Izv. Akad. Nauk SSSR, MZG, No. 6 (1983).